Optics Letters

# High-sensitivity dynamic detection by tapping-mode nanomechanical sensing using an all-fiber microcantilever probe

Famei Wang,[1] Changrui Liao,[2,*] Liping Hou,[3] Mengqiang Zou,[4] Shen Liu,[2] Chao Liu,[5] Paul K. Chu,[6] Xiaoyang Guo,[1] Zhe Zhang,[1] Cangtao Zhou,[1] and Shuangchen Ruan[1]

[1]Shenzhen Key Laboratory of Ultra-Intense Laser and Advanced Material Technology, Center for Intense Laser Application Technology, and College of Engineering Physics, Shenzhen Technology University, Shenzhen 518118, China
[2]Shenzhen Key Laboratory of Ultrafast Laser Micro/Nano Manufacturing, Key Laboratory of Optoelectronic Devices and Systems of Ministry of Education/Guangdong Province, College of Physics and Optoelectronic Engineering, Shenzhen University, Shenzhen 518060, China
[3]Beidahuang Industry Group General Hospital, Heilongjiang, Harbin 150088, China
[4]Chongqing Key Laboratory of Autonomous Navigation and Microsystems, School of Electronic Science and Engineering, Chongqing University of Posts and Telecommunications, Chongqing 400065, China
[5]School of Electronics Science, Northeast Petroleum University, Daqing 163318, China
[6]Department of Physics, Department of Materials Science and Engineering, and Department of Biomedical Engineering, City University of Hong Kong SAR, Tat Chee Avenue, Kowloon, Hong Kong, China
*cliao@szu.edu.cn

Received 30 September 2025; revised 10 November 2025; accepted 10 November 2025; posted 12 November 2025; published 20 November 2025

**In the quest for precise microscale material characterization, the development of high-performance sensors has become a pivotal research area. This study reports what we believe to be the first development of a dynamic microforce sensor that integrates a fiber-optic microcantilever probe operating in tapping-mode atomic force microscopy (AFM). By using femtosecond laser two-photon polymerization (TPP) nanolithography, the microstructure cantilever beam probes are prepared on the fiber end faces. Finite element analysis is performed to determine the dynamic mechanical properties of the optical fiber microcantilever, and the structure is optimized by parametric modeling. The optimized sensor shows a microforce sensitivity of 103 Hz/nm, a quality factor (Q) of 326.98, and a pN-level force detection limit ( 17 pN). Owing to the simple structure and parallel probe configuration, the integrated sensor offers is highly promising in applications such as the quantitative analysis of viscoelastic properties of soft materials and biological samples.** 

https://doi.org/10.1364/OL.580667

Nanotechnology advances materials science, biomedicine, and microelectronics, relying on micro/nanoscale characterization of soft polymers, biological membranes, and metastable nanostructures [1–3]. Atomic force microscopy (AFM) enables atomic-resolution imaging and real-time nanomechanical monitoring [4–6], but suffers from bulky free-space optics, poor photonic integration, and invasive tip–sample contact that may denature biomolecules or deform polymers [7–9]. These limitations drive demand for miniaturized, non-destructive, high-sensitivity sensing platforms.

Optical fiber-based force sensors offer a promising alternative, with EMI immunity, compactness, and compatibility with microfluidic/optical systems [10–13]. Recent designs include interferometric, spectroscopic, and metamaterial-based schemes—e.g., fiber-tip Fabry–Pérot interferometers (FPIs) and 3D-printed probes have achieved pN-level static force detection [14–18]. However, most operate in static contact mode, problematic for soft specimens [19–21], and dynamic modes like AFM tapping—critical for low-contact, high-resolution measurement—remain underdeveloped in fiber systems.

Here, we introduce a dynamically driven fiber-optic microcantilever system that combines tapping-mode operation with interferometric force sensing. Using external optical excitation and phase-sensitive resonance detection, the system attains a force sensitivity of 103 Hz/nm and a quality factor of 326.98, while avoiding bulky optics. Controlled tip–sample engagement enables gentle, high-resolution mapping of soft materials. We establish a correlation between cantilever spring constants and force–distance profiles, providing a quantitative framework for nanomechanical analysis. This work opens a path toward portable, high-sensitivity characterization of biological and polymeric nanomaterials with minimal perturbation.

As shown in Fig. 1(a), the F–P sensor comprises a single-mode fiber (SMF) and a microcantilever assembled on the fiber end face, forming an FPI between the fiber end face and the cantilever's lower surface, where the cavity length critically impacts

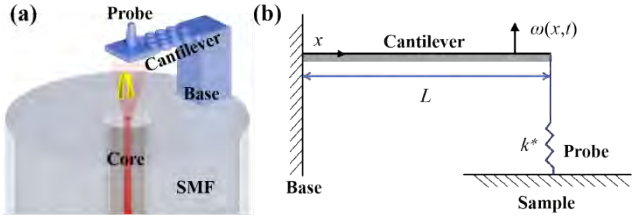


**Fig. 1.** (a) Schematic diagram of the interference principle of the fiber end face FPI and (b) contact resonance mechanics model of the cantilever beam probe.

performance. To improve the sensitivity of the sensor while obtaining high contrast interference spectra, Eq. (1) is used [20]:

$$FSR = \frac{\lambda^2}{2nL}, \tag{1}$$

where λ is the resonant wavelength, $L$ is the cavity length of the F–P cavity, and $n$ is the refractive index of the F–P cavity medium.

When the probe is subjected to a force, the microcantilever beam bends, altering the optical path difference of the F–P cavity and shifting the interference fringes. The deflection of the microcantilever can be determined by detecting the resonant wavelength of the peak or valley in the interference spectrum. The corresponding relationship between the wavelength change ($\Delta\lambda$) and cavity length of the F–P cavity change ($\Delta L$) can be simplified as follows [20]:

$$\frac{\Delta\lambda}{\lambda} = \frac{\Delta L}{L}. \tag{2}$$

The fiber end microcantilever probe is a viable optical demodulation scheme to replace the complex optical lever demodulation method of commercial AFM for better function integration. In addition, the microcantilever structure with one end fixed and the other end suspended, together with the low Young's modulus of polymer materials, enables the microcantilever probe to undergo enough deformation when subjected to a weak force, thereby resulting in a lower force detection limit.

In dynamic-mode atomic force microscopy (AFM), intermittent tip–sample contact reduces sample damage compared to static contact mode. A resonating microcantilever is driven by an external periodic excitation, and its amplitude, phase, or frequency shifts in response to tip–sample forces, enabling surface topography reconstruction. Two common detection schemes are amplitude modulation (AM) and frequency modulation (FM). In FM–AFM, the frequency shift relative to the free resonance serves as the feedback signal, enabling atomic-resolution imaging in ultrahigh vacuum or liquid across various materials.

As shown in Fig. 1(b), the fiber with the cantilever probe is inserted into a ceramic core fixed atop a piezoelectric plate, establishing well-defined resonance boundary conditions. A contact resonance model is developed where the probe–sample interaction is modeled as a spring element with contact stiffness $k^*$. The corresponding resonant frequency $f^*$ and stiffness can be derived from vibration theory as follows [22]:

$$f^* = f_0\sqrt{\frac{k_c + k^*}{k_c}}\sqrt{1 - \frac{1}{2Q^2}}, \tag{3}$$

where $f_0$ is the natural vibration frequency of the cantilever probe, $k_C$ is the spring constant of the cantilever, and $Q$ is the quality factor. By measuring the change of resonance frequency, the change of the spring constant under the contact between the cantilever probe and the sample can be obtained, and the force between the cantilever probe and the sample can be obtained.

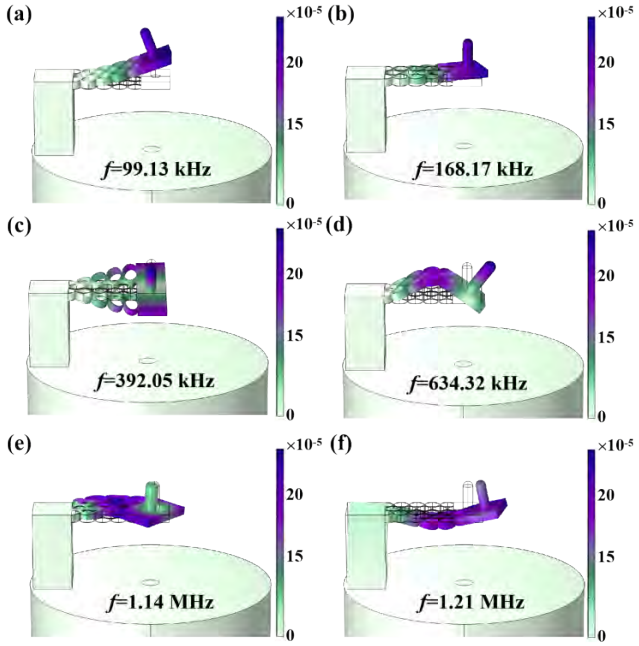


**Fig. 2.** Vibration modal analysis of microcantilever beam probe.

To investigate the dynamic mechanical properties of the fiber-tip microcantilever, a finite element model was established using COMSOL Multiphysics. The polymer probe has a density of 1,499 kg/m³, Young's modulus of 2.34 GPa, and Poisson's ratio of 0.33, while the silica fiber has corresponding values of 2,700 kg/m³, 73 GPa, and 0.17. The cantilever has a width of 22.5 μm, a thickness of 4 μm, a length of 55 μm, a probe height of 10 μm, the rounded corner diameter of the probe tip is 5 μm and a cavity length of 30 μm. Figure 2(a) shows the mode shape of its first-order mode. The microcantilever deflects above the fiber core with a fundamental frequency of 99.13 kHz. The simulated quality factor ($Q$) was calculated via complex eigenvalue theory: using an eigenvalue solver, $\omega = \omega_r + i\omega_i$($\omega_r$: real part of 99.13 kHz, $\omega_i$: imaginary part of 0.1245 kHz) gives $Q = \omega_r/(2\omega_i)$ = 398.11. In the higher-order modes, twisting occurs in the microcantilever probe as it deflects away from the fiber core direction. As shown in Figs. 2(b)–2(f), the high-order resonant frequencies are 168.17 kHz, 392.05 kHz, 634.32 kHz, 1.14 MHz, and 1.21 MHz.

The fiber-tip microcantilever force sensor is fabricated via femtosecond laser two-photon polymerization (TPP). A hollow-structured cantilever design is translated into slicing and motion control parameters, with laser processing performed at 30 mW power, 80 MHz repetition rate, and 800 nm wavelength. Optimized writing parameters (scan speed: 800 μm/s, line and layer spacing: 200 nm) ensure high printing quality. After exposure, cross-linking forms a stable polymer structure bonded firmly to the fiber end face. The sample is developed in PGMEA (≥10 min) and isopropanol ( 5 min), followed by UV post-curing to enhance mechanical stability.

Figures 3(a) and 3(b) show SEM images of the hollow microcantilever, exhibiting a smooth surface and high parallelism to the fiber end, which enhances reflectivity and force sensi-

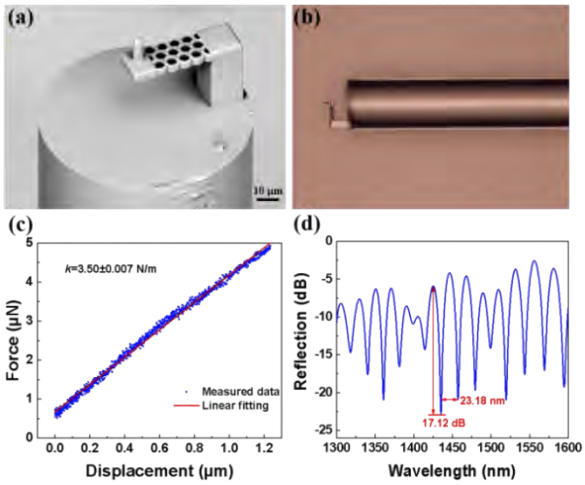


**Fig. 3.** (a) SEM image of fiber end face microcantilever probe; (b) side microscopic image of fiber end face microcantilever probe; (c) force displacement curve of fiber end face microcantilever probe; (d) reflection spectrum of the sensor when no external vibration is applied.

tivity. The reflection spectrum in Fig. 3(d) displays three-beam interference from the fiber end and cantilever surfaces, with an FP envelope near 1435.4 nm (FSR = 23.18 nm, ER = 17.12 dB). Based on Eq. (1), the cavity length is calculated as 22.5 μm; its deviation from design stems from intentional recessed printing (starting 15 μm inside the fiber) to ensure adhesion, with the cantilever's initially designed 55 μm base theoretically yielding a 30 μm distance between the fiber end face and the cantilever's lower surface. However, unavoidable minor errors during manual positioning of the fiber end face led to the discrepancy between this calculated actual cavity length and the theoretical design. Nanoindentation (Hysitron ti980) gives a spring constant of 3.50 N/m (Fig. 3(c)), confirming suitable mechanical properties for microforce sensing.

For dynamically modulated FPI signals—such as those from ultrasonic or low-frequency vibrations-static wavelength-based demodulation becomes inadequate. Instead, dynamic (linear) demodulation offers rapid response and broad frequency range. As illustrated in Fig. 4, a tunable laser source (TLS) with a power of 18 mW and a linewidth of <10 kHz emits light through a circulator into the FPI sensor. The reflected signal is directed to a photodetector (PD) with a bandwidth of 100 Hz–15 MHz and analyzed using a vector network analyzer (VNA) to extract vibration information. External acoustic excitation periodically modulates the FPI cavity length, inducing spectral shifts that are converted by the PD into electrical signals. A piezo-driven stage positions the cantilever probe, while a 3D stage and CCD camera facilitate sample alignment and real-time observation. The entire setup is placed on a vibration-isolation platform within a temperature- and humidity-stabilized cleanroom to minimize environmental disturbances.

In dynamic sensing tests, the fiber with the cantilever probe is fixed via a ceramic plug onto a piezoelectric (PZT) plate. Driven by an AC signal from a signal generator (SG), the PZT excites cantilever vibration, while a PC controls a 3D stage for positioning. A broadband frequency sweep (0–1 MHz) reveals a resonance near 130 kHz (Fig. 5(a)), and a refined sweep (110–150 kHz) identifies the fundamental resonance at 130.79 kHz (Fig. 5(b)). To minimize measurement error

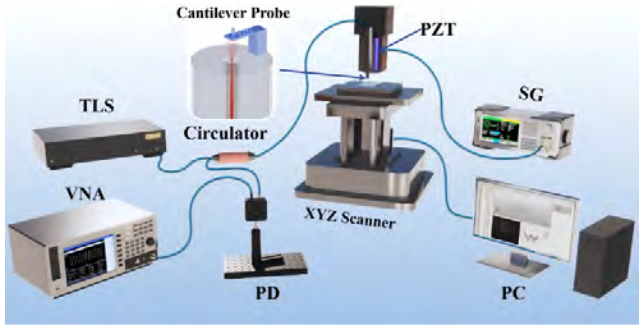


**Fig. 4.** Schematic of the optical fiber end microcantilever dynamic sensing system.

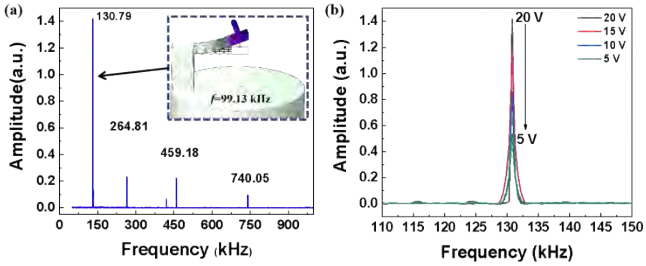


**Fig. 5.** (a) Frequency spectra of fiber end face microcantilever beams in different frequency ranges; (b) spectrum diagram of fiber end face microcantilever beam at different voltages.

caused by weak vibration amplitudes, the excitation voltage is optimized. As shown in Fig. 5(b), increasing the voltage from 5 to 20 V enhances vibration intensity and reduces the resonance linewidth, improving detection accuracy. Accordingly, all subsequent sensing measurements employ a 20 V excitation to ensure reliable probe response. The quality factor is 326.98 at 130.79 kHz, slightly lower than the simulated 398.11 due to practical damping unaccounted for in simulations (air viscous damping, intrinsic photoresist damping, mounting losses, and minor FP optical losses). This discrepancy is reasonable and does not affect performance.

Under external excitation, atomic interactions alter the probe's amplitude, phase, and resonance frequency as it approaches the sample (Fig. 6(a)). Oscillation amplitude remains nearly constant at 60–80 nm separation (negligible van der Waals forces, free oscillation), while below 60 nm, van der Waals forces reduce amplitude progressively; interatomic distances induce rapid damping via repulsive/adhesive forces, validating the theoretical model [22]. Experimentally, the system achieves a microforce sensitivity of 103 Hz/nm ($R^2 = 0.9988$, Fig. 6(b)), with error bars reflecting the standard deviation of three repeated measurements (good repeatability). A frequency noise floor of 0.5 Hz (RMS) in a stabilized environment yields a minimum detectable distance of 4.9 pm and force detection limit of 17 pN. Three temperature rise-fall cycles (humidity-stabilized) show <±1 Hz resonant frequency fluctuation (negligible thermal drift), while resonant intensity decreases at 0.01866 a.u./°C- attributed to enhanced photoresist intrinsic damping, air viscous damping, and minor FP optical coupling attenuation. Operating within the linear elastic regime ensures force–cavity length response without hysteresis, allowing sample topography to be reconstructed from probe height at a fixed frequency offset. The frequency–modulation mode is compatible with ultrahigh vacuum and liquid

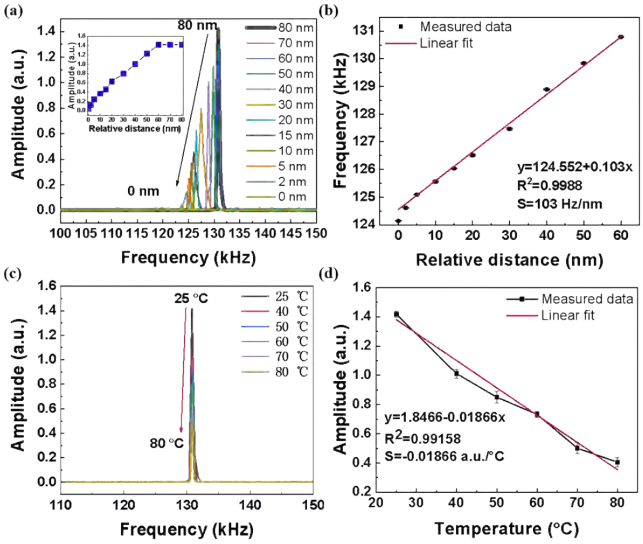


**Fig. 6.** (a) Probe sample spectra at different distances and (b) linear fitting of between spectral variables and distance; (c) probe sample spectra at different temperatures, and (d) linear fitting of between spectral variables and temperatures.

environments, supporting atomic-resolution imaging of metals, semiconductors, and insulators. To confirm the superiority of our device in dynamic operation mode (tapping mode AFM), a detailed performance comparison was made with the recent micro force sensor (Table S1 of Supplement 1).

We demonstrate a dynamically driven fiber-optic microcantilever sensor operating in tapping mode for the first time, fabricated via femtosecond laser two-photon polymerization on a single-mode fiber tip. Finite element analysis guided structural optimization, yielding a microforce sensitivity of 103 Hz/nm and a quality factor of 326.98, and a pN-level force detection limit ( 17 pN). The sensor has the advantages of a small size, no special packaging requirements, good biocompatibility, and all-fiber operation. The optical fiber nanodynamic mechanical sensor described here enables simple and parallel determination of the mechanical properties of materials, especially soft and biological samples. As a result, the device has large potential as a nano dynamic mechanical sensor in many biological and medical applications, such as microbial activity assessment.

**Funding.** National Natural Science Foundation of China (62305223, 62405040); Shenzhen Science and Technology Innovation Program (ZDSYS20220606100405013); the Guangdong Province Key Construction Discipline Scientific Research Capacity Improvement Project (2021ZDJS107); China Postdoctoral Science Foundation (2025M770851); the Chongqing Postdoctoral Research Project Special Funding (2024CQBSHTB3070); Natural Science Foundation of Heilongjiang Province (JQ2023F001); City University of Hong Kong Donation Research Grants (9220061, DON-RMG 9229021).

**Disclosures.** The authors declare no conflicts of interest.

**Data availability.** Data underlying the results presented in this paper are not publicly available at this time but may be obtained from the authors upon reasonable request.

**Supplemental document.** See Supplement 1 for supporting content.

## REFERENCES

1. J. N. Hong, Y. Tian, T. C. Liang, *et al.*, Nature. **630**, 375 (2024).
2. H. W. Seo, J. U. Lee, C. H. Yang, *et al.*, J. Korean Phys. Soc. **80**, 1035 (2022).
3. R. Baez-Cruz, R. Sekar, and P. Manidurai, Nano **18**, 2350016 (2023).
4. M. Bina, A. Krywko-Cendrowska, D. Daubian, *et al.*, Nano Lett. **22**, 5077 (2022).
5. P. Zamprogno, G. Thoma, V. Cencen, *et al.*, ACS Biomater. Sci. Eng. **2997**, 2990 (2021).
6. C. Yilmaz, J. Braz. Soc. Mech. Sci. Eng. **46**, 398 (2024).
7. N. F. Faruk, X. D. Peng, and T. R. Sosnick, Int. J. Mol. Sci. **24**, 2654 (2023).
8. M. Q. Zou, C. R. Liao, Y. P. Chen, *et al.*, Int. J. Extrem. Manuf. **5**, 015005 (2023).
9. V. Vahdat and R. W. Carpick, ACS Nano **7**, 9836 (2013).
10. Y. Chen, S. C. Yan, X. Zheng, *et al.*, Opt. Express **22**, 2443 (2014).
11. H. Qian, J. Lee, F. T. Arce, *et al.*, Nat. Photon. **11**, 352 (2017).
12. S. Pevec and D. Donlagic, Opt. Lett. **45**, 5093 (2020).
13. W. Bao, X. Li, F. Chen, *et al.*, J. Lightwave Technol. **40**, 4020 (2022).
14. Y. Gong, C. B. Yu, T. T. Wang, *et al.*, Opt. Express **22**, 3578 (2014).
15. M. Q. Zou, C. R. Liao, S. Liu, *et al.*, Light Sci. Appl. **10**, 171 (2021).
16. X. G. Shang, N. Wang, and Z. M. Qiu, Adv. Mater. **36**, 2305121 (2024).
17. F. M. Wang, M. Q. Zou, C. R. Liao, *et al.*, APL Photon. **8**, 096108 (2023).
18. F. M. Wang, C. R. Liao, M. Q. Zou, *et al.*, Photonics Sens. **14**, 240204 (2024).
19. C. Hong, J. Huang, W. Chen, *et al.*, Soil Till. Res. **234**, 105834 (2023).
20. M. Q. Zou, C. R. Liao, Y. P. Chen, *et al.*, Biosens. **12**, 629 (2022).
21. P. Bian, Z. Y. Hu, R. An, *et al.*, Laser Photon. Rev. **18**, 2300957 (2024).
22. X. H. Gu, L. N. Sun, and C. H. Ru, Eur. Phys. J-Appl. Phys. **82**, 10701 (2018).

Supplemental document accompanying submission to *Optics Letters*

**Title:** High-sensitivity dynamic detection by tapping-mode nanomechanical sensing using an all-fiber microcantilever probe

**Authors:** Changrui Liao, Famei Wang, Liping Hou, Mengqiang Zou, Shen Liu, Chao Liu, Paul Chu, Xiaoyang Guo, Zhe Zhang, Cangtao Zhou, Shuangchen Ruan

**Submitted:** 9/29/2025 9:29:39 PM

**Supplementary Information**

# High-Sensitivity Dynamic Detection by Tapping-Mode Nanomechanical Sensing Using an All-Fiber Microcantilever Probe

**FAMEI WANG,[1] CHANGRUI LIAO,[2,*] LIPING HOU,[3] MENGQIANG ZOU,[4] SHEN LIU,[2] CHAO LIU,[5] PAUL K. CHU,[6] XIAOYANG GUO,[1] ZHE ZHANG,[1] CANGTAO ZHOU,[1] AND SHUANGCHEN RUAN,[1]**

*[1] Shenzhen Key Laboratory of Ultra-Intense Laser and Advanced Material Technology, Center for Intense Laser Application Technology, and College of Engineering Physics, Shenzhen Technology University, Shenzhen 518118, China*
*[2] Shenzhen Key Laboratory of Ultrafast Laser Micro/Nano Manufacturing, Key Laboratory of Optoelectronic Devices and Systems of Ministry of Education/Guangdong Province, College of Physics and Optoelectronic Engineering, Shenzhen University, Shenzhen 518060, China*
*[3] Beidahuang Industry Group General Hospital, Heilongjiang, Harbin 150088, China*
*[4] Chongqing Key Laboratory of Autonomous Navigation and Microsystems, School of Electronic Science and Engineering, Chongqing University of Posts and Telecommunications, Chongqing 400065, China*
*[5] School of Electronics Science, Northeast Petroleum University, Daqing 163318, P.R. China*
*[6] Department of Physics, Department of Materials Science and Engineering, and Department of Biomedical Engineering, City University of Hong Kong, Tat Chee Avenue, Kowloon, Hong Kong, China*
**cliao@szu.edu.cn*

Received XX Month XXXX; revised XX Month, XXXX; accepted XX Month XXXX; posted XX Month XXXX (Doc. ID XXXXX); published XX Month XXXX

## S1. Performance Comparison

As shown in Table I, when compared with previous microforce sensors, the optical fiber sensor described in this paper shows superior sensitivity and other advantages that include high Q-Factor, force sensitivity, and ultra-low force resolution. The resulting force detection limit down to 17 pN, which is much lower than that reported previously for any other optical fiber microforce sensors. The proposed optical fiber force sensor is applicable to measurement of weak forces of the order of piconewtons (pN) for biological samples.

**Table I. Performance Comparison of Microforce Sensors**

| Sensor Type | Operating Mode | *f*(kHz) | Q-Factor | Force Sensitivity | Resolution/ Detection limit | Refs. |
|---|---|---|---|---|---|---|
| Traditional AFM cantilever | Dynamic | 195 | 10.4 | - | - | [1] |
| Traditional AFM cantilever | Dynamic | 15.2 | 300 | - | - | [2] |
| ROTMO | Dynamic | 233.6 | 95 | - | - | [3] |
| F-P Acoustic Sensor | Dynamic | 10 | - | 1100 nm/kPa | 60 μPa/Hz | [4] |
| Nanoresonator with MLG Film | Dynamic | 135 | 81 | 3.8 fN/Hz | - | [5] |
| Clamped beam probe fiber FPI | Static | - | - | 1.51 nm/μN | 55 nN | [6] |
| PDMS fiber FPI | Static | - | - | 45.72 nm/μN | 0.44 nN | [7] |
| FONP | Static | - | - | 54.5 nm/μN | 2.1 nN | [8] |
| **Microcantilever FPI** | Dynamic | 130.79 | 326.98 | 103 Hz/nm | **0.017 nN** | **This work** |


1. P. I. Dietrich, G. Goring, M. Trappen, M. Blaicher, W. Freude, T. Schimmel, H. Holscher, C. Koos,3D-Printed Scanning-Probe Microscopes with Integrated Optical Actuation and Read-Out, Small, 16, 1904695(2020).
2. B. Pottier, L. Bellon, Force microscopy cantilevers locally heated in a fluid: Temperature fields and effects on the dynamics, J. Appl. Phys. 130, 124502 (2021).
3. S. Pevec and D. Donlagic, Resonant-Opto-Thermomechanical Oscillator (ROTMO): A Low-Power, Large Displacement, High-Frequency Optically Driven Microactuator, Small, 18, 2107552 (2022).
4. J. Ma, H.F. Xuan, H.L. Ho, W. Jin, Y.H. Yang, and S.C. Fan, Fiber-Optic Fabry–Pérot Acoustic Sensor With Multilayer Graphene Diaphragm, IEEE PHOTONICS TECHNOLOGY LETTERS, 25(10), 932-935(2013).
5. J. Ma, W. Jin, H.F. Xuan, C. wang, and H.L. Ho, Fiber-optic ferrule-top nanomechanical resonator with multilayer graphene film, Opt. Lett. 39(16), 4769-4772(2014).
6. M.Q. Zou, C.R. Liao, S. Liu, C. Xiong, C. Zhao, J. Zhao, Z.S. Gan, Y. Chen, K. Yang, and D. Liu, Fiber-tip polymer clamped-beam probe for high-sensitivity nanoforce measurements, Light Sci. Appl. 10, 171 (2021).
7. W.J. Bao, X.Y. Li, F.Y. Chen, R.H. Wang, and X.G. Qiao, Hyperelastic Polymer Fiber Fabry–Pérot Interferometer for Nanoforce Measurement, J. Lightwave Technol. 40(12), 4020-4026 (2022).
8. M.Q. Zou, C.R. Liao, Y.P. Chen, L. Xu, S. Tang, G.X. Xu, Ke Ma, J.T. Zhou, Z.H. Cai, B.Z. Li, C. Zhao, Z.R. Xu, Y.Y. Shen, S. Liu, Y. Wang, Z.S. Gan, H. Wang, X.M. Zhang, S. Kasas, and Y.P. Wang, 3D printed fiber-optic nanomechanical bioprobe, Int. J. Extrem. Manuf. 5, 015005 (2023).